Proceedings of the 17th World Congress
The International Federation of Automatic Control
Seoul, Korea, July 6-11, 2008

TELEDIAGNOSIS OF TRANSMISSION CHANNEL AND ACTUATORS FAULTS ON A MOBILE ROBOT

K. Fawaz, R. Merzouki, B. Ould Bouamama

LAGIS, UMR CNRS 8146, Ecole Polytechnique de Lille, Avenue Paul Langevin, 59655 Villeneuve d'Ascq, France.
khaled.fawaz@polytech-lille.fr

Abstract: This paper deals with a model based fault detection and isolation (FDI) approach in order to detect and to isolate the transmission channel fault from the actuators faults of a mobile robot. A Co-simulation with virtual robot is developed, allowing to understand the faults influences on the synthesized residuals. Simulation and experimental results show clearly the isolability between the studied faults. *Copyright © 2008 IFAC*

Keywords: Fault Detection & Isolation (FDI), Co-Simulation, Transmission Channel, Mobile Robot, Modelling.

1. INTRODUCTION

Actually, the major trend in performing a modern industrial system is the ability to control, supervise and maintenance all its components. More and more that the controlled systems are taken certain autonomy of operation, then they should be perfectly supervised and maintained at distance via a transmission channel. Many works have been done on the distributed control systems during the last decade as in Zheng *et al.* (2006), where a Takagi--Sugeno (T--S) model is used to represent a networked control system (NCS) with different network-induced delays. Comparing with existing NCS modeling methods, this approach addresses situations involving all possible network-induced delays. Moreover, this approach also handles data-packet loss. For the FDI problematic, a parity-equation approach and a fuzzy-observer-based approach for fault detection of an NCS are developed. Then, Kalman filters are constructed for NCS in Zheng2 *et al.* (2004) according to different system faults. In *Magni & Mouyon* (1994), the parity-equation approach and the observer-based approach are used for residual generation. In *Ye et al.* (2004), the introduction of the so-called stationary wavelet transform into the residual signal for residual generator, shows a new approach which ensures a good performance index, a satisfactory low misdetection rate and a suitable response speed to faults with a low order parity vector and a simple online implementation form. Among some results related to diagnosis of actuators faults, in *Merzouki et al.* (2007), a contribution on how to detect and to localize the failures introduced by the mechanical backlash is proposed. The main purpose is to distinguish the disturbing backlash from the useful one during a normal operation of the electromechanical system, while in *Djeziri et al.* (2007), the residuals and the thresholds are generated in presence of parameter uncertainties, using bond graph representation under linear fractional transformation form (LFT), and applied for a mechatronic system. The whole of : nonlinear system model, structural analysis, residual with adaptive thresholds generations, and residual sensitivity analysis, are synthesized using the bond graph properties.

One of the principle component of the NCS is the transmission channel, which is defined as a link between two communicant systems, and it is modelled by different manners according to the applications. In the framework of the information theory, it is regarded as a source of corruption *Shannon* (1949). Furthermore, in control field, it is considered as a source of the communication time delay. The main problem in this case is the development of an appropriate delay model which takes into account the existing system. In *Miano & Mafucci* (2001), a description of different types of transmission line without losses is presented and in *Witrant* (2005) a nonhomogeneous model of a transmission line is developed by using the Bond graph model, while other approaches use the transmission channel as a variable time delay *Krtolica et al.* (1994), *Nilsson* (1998).

In this paper, a Co-simulation between a virtual and a real mobile robot is presented. It concerns the on line telediagnosis of transmission channel and actuators faults of a mobile robot. Two innovated points are given through this work: the first concerns the transmission channel which is considered as a uncoupled system, modelled separately from the robot model, and concatenated to this latter for the FDI algorithm synthesis. The second point relates to the development of a virtual simulator which can work in parallel with the real robot. The interest of this simulator is its ability to inform the system supervisor of any transmission and/or actuators faults, without being closer to the real system. The word 'telediagnosis' explains that the

FDI algorithm uses only the sensor data transmitted via the transmission channel (RS232 cable), while the controller data are locally to the robot system.
This paper is organized as follows: after the introduction section, a modeling step of the whole of the transmission channel and the mobile robot is given in Section 2. Section 3 presents the Fault Detection and Isolation (FDI) algorithm. Section 4 is devoted to simulation and experimental results done on the mobile robot system.

2. DYNAMIC MODEL OF GLOBAL SYSTEM

In this section, a description of the principal studied system parts is introduced. Also, the modelling of the transmission channel and the miniature mobile robot is presented.

2.1 Robot System Description

The studied mobile robot Khepera II *K-Team*, is a double active wheeled and miniature robot Fig. 1 (a).

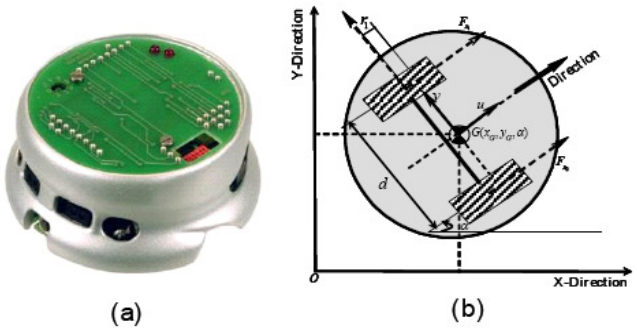

Fig. 1 (a): Khepera II robot - (b): Robot description schema

Each wheel is moved by a DC motor coupled with the wheel through a 25:1 reduction gearbox. An incremental encoder, placed on the motor axis, gives 24 pulses per revolution of the motor. This allows a resolution of 600 pulses per revolution of the wheel that corresponds to 12 pulses per millimeter of path of the robot. The motor controller can be used in two control modes (Fig. 2) The velocity and the position modes. The active control mode is set according to the kind of command received. If the controller receives a velocity control command, it switches to the velocity mode. If the controller receives a position control command, the control mode is automatically switched to the position mode. Different PID control parameters (K_p, K_I and K_D) can be set for each of the two control modes. This robot is controlled via a serial transmission channel (Fig. 2), where the desired position and desired velocity values are introduced outside the robot system.

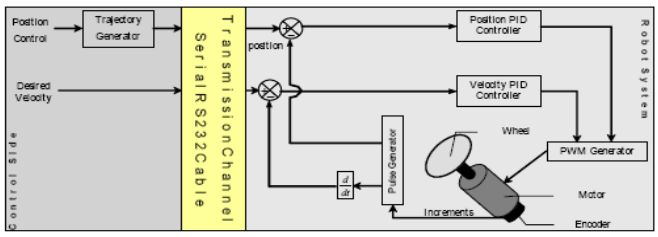

Fig. 2 Position and velocity Controls Schema

2.2 Robot Modelling

Some hypotheses are taken in consideration for these parts according to the robot characteristics and its environment:
1. The contact area between robot wheels and the motion surface is assimilated to a point contact, due to the rigidity of the robot wheel;
2. The contact efforts are considered static in function of the time, due to the homogeneous of the contact area. These efforts are taken as a system inputs;
3. For the miniature robot actuators, only the mechanical dynamic part is considered, the parameters of the electrical part are neglected;
4. For dynamic robot modeling, only longitudinal and yaw dynamics are studied. The lateral dynamic is neglected due to the minor lateral efforts on the robot dynamic motion, issued from a so small width of the wheels.

Kinematic Model: Fig. 1(b) shows the robot centre of mass $G(x_G, y_G, \alpha)$, where (x_G, y_G) are the absolute coordinates and α the yaw angle. When the static radius of the robot wheel is R and the measured wheel velocities $\dot{\theta}_1$ and $\dot{\theta}_2$, then the deduced kinematic model of the robot is given as follows:

$$\begin{pmatrix} \dot{u} \\ \dot{v} \\ \dot{\alpha} \end{pmatrix} = \begin{pmatrix} R/2 & R/2 \\ (R.r_1)/2 & -(R.r_1)/2 \\ R/d & -R/d \end{pmatrix} . \begin{pmatrix} \dot{\theta}_1 \\ \dot{\theta}_2 \end{pmatrix} \quad (1)$$

with: $\dot{u}$ the longitudinal velocity of the centre of mass, $\dot{v}$ the lateral velocity of the centre of mass, $\dot{\alpha}$ the yaw velocity, d the normal distance between the wheels and r_1 the distance between the wheel axis and the centre of the mass.

Geometric Model: These model concerns the deduction of the (x_G, y_G) coordinates at the absolute reference (Fig. 1(b)). Thus, from equations (1) and after geometrical projection, this following system of equations is obtained:

$$\begin{cases} x_G = \int (\dot{u}.cos\alpha - \dot{v}.sin\alpha)dt + x_{G0} \\ y_G = \int (\dot{u}.sin\alpha + \dot{v}.cos\alpha)dt + y_{G0} \end{cases} \quad (2)$$

Where: (x_{G0}, y_{G0}) are deduced from initial conditions.

Dynamic Model: In this model, dynamics related to the mechanical part of the actuators, to the longitudinal motion and to the yaw motion are developed, using the fundamental law of dynamic. Then, the following system of equations regroups these four dynamics:

- *Longitudinal dynamic*:

$$F_{x1} + F_{x2} - f_m.\dot{u} = m.\ddot{u} \quad (3)$$

- *Yaw dynamic*

$$(F_{x1} + F_{x2}).\frac{d}{2} - f_z.\dot{\alpha} = I_z.\ddot{\alpha} \quad (4)$$

- *Mechanical dynamic of actuator1*

$$U_1 - f_1.\dot{\theta}_1 - R.F_{x1} = J_1.\ddot{\theta}_1 \quad (5)$$

- *Mechanical dynamic of actuator2*

$$U_2 - f_2.\dot{\theta}_2 - R.F_{x2} = J_2.\ddot{\theta}_2 \quad (6)$$

Where: F_{x1} and F_{x2} are respectively the longitudinal efforts, U_1 and U_2 are the control inputs, m is the robot mass, f_1, J_1, f_2, J_2 are respectively the viscous friction parameters

and the inertias of the two wheel actuators, f_m, f_z are the viscous friction and the flexion parameters of the robot. $\ddot{u}, \ddot{\alpha}, \ddot{\theta}_1, \ddot{\theta}_2, \dot{u}, \dot{\alpha}, \dot{\theta}_1, \dot{\theta}_2$ are the longitudinal, the yaw and the two rotational accelerations and velocities of the wheels. As it is mentioned at the introduction of this section, the longitudinal efforts are supposed as a system inputs.
Then, the state representation of the robot system is the following:

$$\begin{cases} \begin{pmatrix} \ddot{u} \\ \ddot{\alpha} \\ \ddot{\theta}_1 \\ \ddot{\theta}_2 \end{pmatrix} = \begin{pmatrix} 0 & 0 & \frac{-f_m}{m} & 0 \\ 0 & 0 & 0 & \frac{-f_z}{I_z} \\ \frac{-f_1}{J_1} & 0 & 0 & 0 \\ 0 & \frac{-f_2}{J_2} & 0 & 0 \end{pmatrix} \cdot \begin{pmatrix} \dot{u} \\ \dot{\alpha} \\ \dot{\theta}_1 \\ \dot{\theta}_2 \end{pmatrix} \\ \quad + \begin{pmatrix} \frac{1}{m} & \frac{1}{m} & 0 & 0 \\ \frac{d}{2I_z} & \frac{-d}{2I_z} & 0 & 0 \\ \frac{-R}{J_1} & 0 & \frac{1}{J_1} & 0 \\ 0 & \frac{-R}{J_2} & 0 & \frac{1}{J_2} \end{pmatrix} \cdot \begin{pmatrix} F_{x1} \\ F_{x2} \\ U_1 \\ U_1 \end{pmatrix} \\ \begin{pmatrix} \dot{\theta}_1 \\ \dot{\theta}_2 \end{pmatrix} = \begin{pmatrix} 0 & 0 & 1 & 0 \\ 0 & 0 & 0 & 1 \end{pmatrix} \cdot \begin{pmatrix} \dot{u} \\ \dot{\alpha} \\ \dot{\theta}_1 \\ \dot{\theta}_2 \end{pmatrix} \end{cases} \quad (7)$$

With: $(\dot{u} \quad \dot{\alpha} \quad \dot{\theta}_1 \quad \dot{\theta}_2)^T$ the state vector, $(\dot{\theta}_1, \dot{\theta}_2)^T$ the outputs vector and $(F_{x1} \quad F_{x2} \quad U_1 \quad U_2)^T$ the inputs vector.

2.3 Transmission Channel Modelling

The used serial line is asynchronous with TTL levels (0-5V). For the studied case, the serial line powers the robot and its length is limited to two meters. Concerning the modelling step, two hypothesis are assumed:
1) According to the cable length, the induced delays are neglected and the data-packet loss are not considered;
2) All external disturbances as noises or equivalent are not considered.
Several transmission channel models are proposed in the literature according to the applications requirements. Among them, in *Teppoz* (2005), an approach taking into account the resistive dissipation and based on a concatenation of basic RLC cells is presented. This approach is used for modelling our two meters length serial cable. It consists on representing the channel as a succession of symmetrical RLC cells, in order to preserve the equality of all the electrical equations for the couple (voltage, current) of each point of the channel, during the transmission time. In Fig. 3(a), a representation on what could be the RLC cell of the length l from the channel, and Fig. 3(b) describes an asymmetric RLC cell, where the basic two elements R_l and L_l are divided in order to create other equivalent elements. Fig. 4 shows the symmetric RLC cell of the l^{th} channel length.

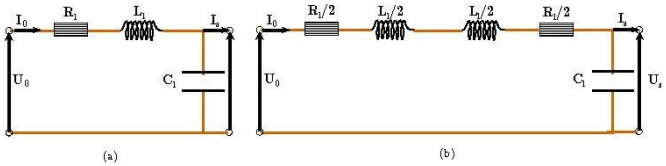

Fig. 3 (a): Standard RLC circuit, (b): Asymmetric RLC cell

The studied serial cable is modelled by only one cell on the whole length. Its correspondent elements are identified experimentally.

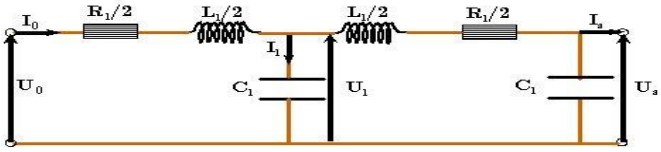

Fig. 4 Symmetric RLC cell

After applying the *Kirchhoff* law on the circuit of Fig. 4, the following system is obtained:

$$\begin{cases} U_0 = U_1 + \frac{R_l}{2}.I_0 + \frac{L_l}{2}.\dot{I}_0 \\ I_0 - I_1 = C_l \dot{U}_1 \\ U_1 = U_s + \frac{R_l}{2}.I_s + \frac{L_l}{2}.\dot{I}_s \\ U_s = R_f.I_s \end{cases} \quad (8)$$

with: l the channel length, R_l, L_l and C_l are respectively the resistance, inductance and the capacity of the cable of length l and they are estimated experimentally according to the cable material' nature. R_f is the internal robot impedance and U_0, U_s are respectively the input and output cable voltages which are experimentally measured. Then, the deduced state representation is given as follows:

$$\begin{cases} \begin{pmatrix} \dot{I}_0 \\ \dot{U}_1 \\ \dot{I}_s \end{pmatrix} = \begin{pmatrix} -\frac{R_l}{L_l} & -\frac{2}{L_1} & 0 \\ \frac{1}{C_l} & 0 & -\frac{1}{C_l} \\ 0 & \frac{2}{L_l} & -\frac{R_l}{L_l} \end{pmatrix} \cdot \begin{pmatrix} I_0 \\ U_1 \\ I_s \end{pmatrix} + \begin{pmatrix} \frac{2}{L_l} \\ 0 \\ 0 \end{pmatrix} . U_0 \\ U_s = (0 \quad 0 \quad R_f) . \begin{pmatrix} I_0 \\ U_1 \\ I_s \end{pmatrix} \end{cases} \quad (9)$$

With: $(I_0 \quad U_1 \quad I_s)^T$ the state vector, U_0 the system input and U_s the system output.

3. FAULT DETECTION AND ISOLATION ALGORITHM

In this section, a model based Fault Detection & Isolation algorithm (FDI) *Staroswiecki & Comtet-Varga* (2001), *Isermann* (1997) is build, in order to detect the transmission channel and actuators fault on the mobile robot system. This detection can help on improving the system performances from a distance.
By using the FDI algorithms proposed in Bouamama *et al.* (2003), a list of Analytical Redundancy Relation (ARR) along with the corresponding Fault Signature Matrix (FSM) can be generated. These tools allow to detect and isolate the possible faults present on the physical system.
The FDI proposed approach is based on the calculation of the residuals issued from the Analytical Redundancy Relation (ARR) and it makes the difference between the dynamic system in normal and faulty situations. Note that for an observable system, with none unresolved algebraic loops, the number of ARR generated are equal to the number of the measured states *Merzouki et al.* (2007). In the studied case, the measured states are the two angular velocities of the wheel and the voltage at the end side of the transmission cable.
The main steps to generate the list of ARR and the FSM by using are summarized below:

- Elimination the unknown variables from each constitutive relation on the dynamic system model.
- Generation of the ARR and the corresponding FSM.

ARR1 Generation

In order to generate the first actuator residual, we eliminate at first the variable F_1, after deducing its expression by adding equations (3) with (4) and substituting with (1)

$$F_1 = R.\begin{bmatrix} \left(\frac{m}{4}+\frac{I_z}{d^2}\right).\ddot{\theta}_1 + \left(\frac{m}{4}-\frac{I_z}{d^2}\right).\ddot{\theta}_2 \\ +\left(\frac{f_m}{4}+\frac{f_z}{d^2}\right).\dot{\theta}_1 + \left(\frac{f_m}{4}-\frac{f_z}{d^2}\right).\dot{\theta}_2 \end{bmatrix} \quad (10)$$

After replacing expression (10) in (5) we obtain the first residual:

$$r_1 = \begin{cases} \left(J_1+\frac{mR^2}{4}+\frac{I_zR^2}{d^2}\right).\ddot{\theta}_1 + \left(\frac{mR^2}{4}-\frac{I_zR^2}{d^2}\right).\ddot{\theta}_2 \\ +\left(f_1+\frac{f_mR^2}{4}+\frac{f_zR^2}{d^2}\right).\dot{\theta}_1 + \left(\frac{f_mR^2}{4}-\frac{f_zR^2}{d^2}\right)\dot{\theta}_2 - U_1 \end{cases} \quad (11)$$

ARR2 Generation

From equations (3) and (4) F_2 can be expressed as follows:

$$F_2 = R.\begin{bmatrix} \left(\frac{m}{4}-\frac{I_z}{d^2}\right).\ddot{\theta}_1 + \left(\frac{m}{4}+\frac{I_z}{d^2}\right).\ddot{\theta}_2 \\ +\left(\frac{f_m}{4}-\frac{f_z}{d^2}\right).\dot{\theta}_1 + \left(\frac{f_m}{4}+\frac{f_z}{d^2}\right).\dot{\theta}_2 \end{bmatrix} \quad (12)$$

After replacing expression (12) in (6), we obtain the second residual:

$$r_2 = \begin{cases} \left(\frac{mR^2}{4}-\frac{I_zR^2}{d^2}\right).\ddot{\theta}_1 + \left(J_2+\frac{mR^2}{4}+\frac{I_zR^2}{d^2}\right).\ddot{\theta}_2 \\ +\left(\frac{f_mR^2}{4}-\frac{f_zR^2}{d^2}\right)\dot{\theta}_1 + \left(f_2+\frac{f_mR^2}{4}+\frac{f_zR^2}{d^2}\right)\dot{\theta}_2 - U_2 \end{cases} \quad (13)$$

ARR3 Generation

From system of equations (8), by substituting the 4^{th} equation in the 3^{rd} the following expression is obtained:

$$U_1 = \left(1+\frac{R_l}{2R_f}\right).U_s + \frac{L_l}{2R_f}.\dot{U}_s \quad (14)$$

then by replacing equation (14) in the 2^{nd} equation of the system (8) we obtain:

$$I_0 = \frac{1}{R_f}.U_s + C_l.\left(1+\frac{R_l}{2R_f}\right).\dot{U}_s + C_l.\frac{L_l}{2R_f}.\dot{U}_s \quad (15)$$

the following residual of the transmission channel with one RLC cell is synthesis after replacing expressions (14) and (15) in the 1^{st} equation of the system (8)

$$r_3 = \begin{cases} \left(\frac{L_lC_l}{4R_f}\right).\dddot{U}_s + \left[\frac{L_l}{R_f}+C_l.\left(1+\frac{R_l}{2R_f}\right)\right].\ddot{U}_s \\ +\left[\left(\frac{L_l+C_l}{2}\right).\left(1+\frac{R_l}{2R_f}\right)+\frac{L_lC_lR_l}{4R_f}\right].\dot{U}_s \\ +\left(1+\frac{R_l}{2R_f}\right).U_s - U_0 \end{cases} \quad (16)$$

In the case of the asynchronous and isolated line with TTL levels, the U_s signal is so clean that it's successively derivatives are not perturbed.

The corresponding FSM of the system under study is given in Table 1.

Table 1 Fault signature matrix of the system

		D_b	I_b	r_1	r_2	r_3
Velocity sensor 1	$\dot{\theta}_1$	1	0	1	1	0
Velocity sensor 1	$\dot{\theta}_1$	1	0	1	1	0
Mechanical part	J_1	1	0	1	0	0
	f_1	1	0	1	0	0
	J_2	1	0	0	1	0
	f_2	1	0	0	1	0
Control Input	U_1	1	1	1	0	0
	U_2	1	1	0	1	0
Cable Voltage	U_s	1	1	0	0	1

In this table, the rows represent the components signatures and the columns are respectively fault detectability D_b fault isolability I_b and first and the three residuals r_1, r_2 and r_3. A '1' value on respectively D_b and I_b columns means that faults on the corresponding components are detectable and isolable. The presence of '1' value on the residual columns shows the influence of the corresponding components on the residual dynamics. In this application, the FSM helps to detect and to distinguish the transmission channel fault from the actuators faults. We can notice that only residual r_3 is sensible to the cable fault, this wants to say that the robot continue moving, in spite of the cable failure, on the other hand it will not receive any more new informations.

4. SIMULATION & EXPERIMENTAL RESULTS

Simulation parameters used for the robot system are given in Table 2. Actuators and cable parameters are given by their notice characteristics, then all the other resistances are identified experimentally. Due to the small values of the parameters, their parameter uncertainties and the models uncertainties are neglected. In order to simulate really a cable fault, a potentiometer of value R_o is connected to the serial cable, in order to vary locally its resistance value. Thus, we can simulate a cut in the cable by increasing the resistance value of R_l, through R_o.

Table 2 Simulation model parameters

Param.	Value	Param.	Value
J_1, J_2	0.1 $(kg.m^2)$	f_m	0.0001 $\left(\frac{N.m.s}{rd}\right)$
f_1, f_2	0.0003 $\left(\frac{N.m.s}{rd}\right)$	f_z	0.0005 $\left(\frac{N.m.s}{rd}\right)$
R	0.005 (m)	r_1	0.01 (m)
d	0.04 (m)	I_z	0.0058 $(kg.m^2)$
R_l	3.2 (Ω)	m	0.250 (kg)
C_l	110.10^{-12} (F)	L_l	250.10^{-9} (H)
R_0	100 (Ω)	R_f	1000 (Ω)

The proposed co-simulation schema is described by Fig 5, where the same input velocities are applied to the both simulator and robot. Then, the whole outputs are exploited by the virtual simulator bloc in order to reconstruct the robot trajectory according to the Cartesian coordinates of the robot. This virtual simulator was built by Virtual Reality Matlab toolbox using the model developed above. The residuals indicate the influence of the studied faults on the global system performances. In the following graphics, we show the time evolution of the inputs and the outputs of the system in normal situation (i.e. without faults) and in faulty situations. In Fig.6 a superposed signals of desired and output velocities for each wheels are presented in normal situation. The regulation is made by the internal robot PID controller of velocity (with: K_p=3790, K_I=803, K_D=104; 1unit=8mm/s), where the controls and residuals signals are given respectively in Fig. 7.and 8 The convergence of the residuals to zero indicates that the global system is in normal situation. In Fig. 9, the desired, simulated and real trajectories are presented. The difference between simulated and experimental trajectories is principally due to the modelling and parameters uncertainties and to the absence of generation

trajectory algorithm, which is not the aim of this work. After simulating an actuator fault by adding a faulty profile in the existing control torque of actuator 1 of Fig. 11, then the velocity tracking of Fig. 10, the residuals of Fig. 12 and the trajectories of Fig. 13 show the influence of the introduced fault on the system performance. However, by introducing a cable fault of Fig. 12, we can notice that only residual r_3 is sensible to this fault (Table 1), because all the regulations are made locally to the robot system and only the input system data are forwarded by the serial cable.

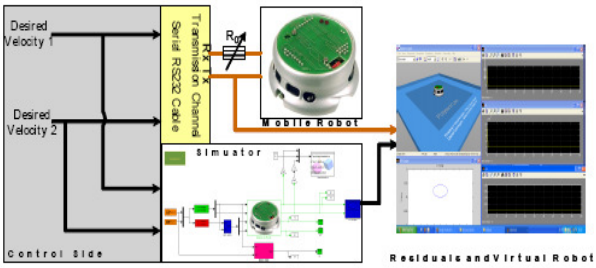

Fig. 5 Co-Simulation robot description

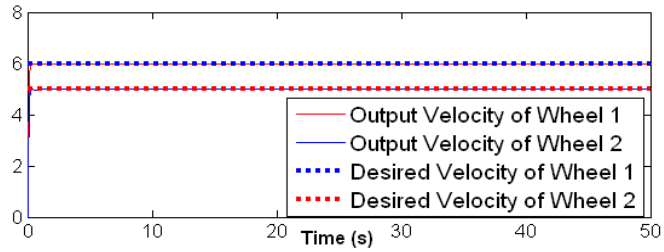

Fig. 6 Desired and output velocities of the wheels in normal situation

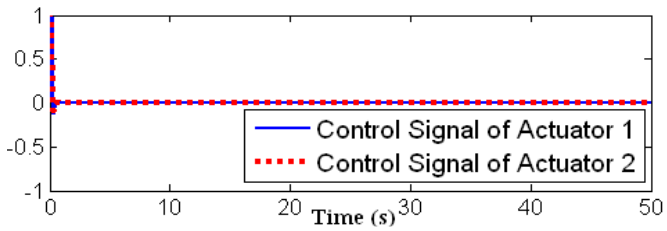

Fig. 7 Actuators control signals in a normal situation

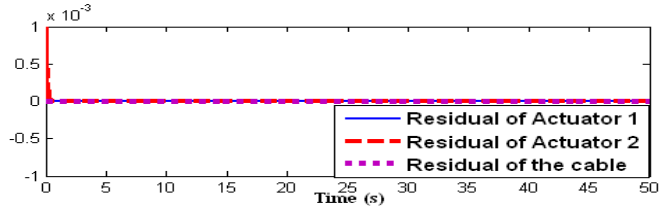

Fig. 8 Residuals r_1, r_2 and r_3 in normal situation

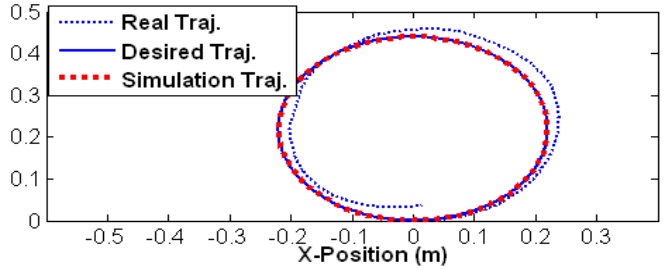

Fig. 9 Desired, simulated and real robot trajectories in normal situation

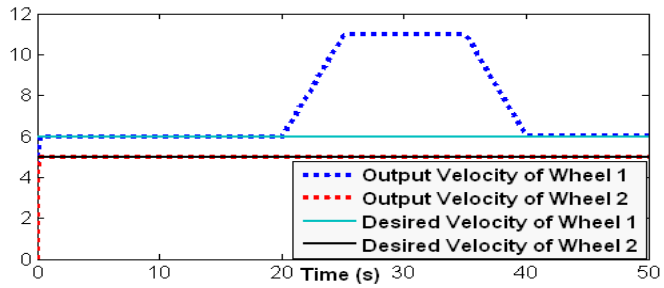

Fig. 10 Desired and output velocities of the wheels in faulty situation

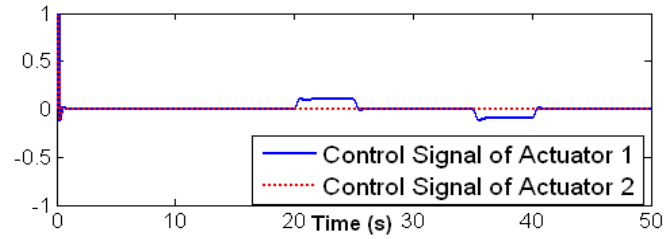

Fig. 11 Actuators control signals in a faulty situation

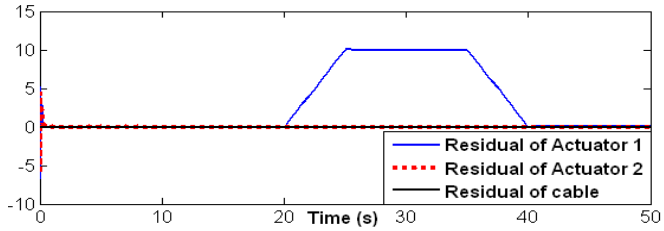

Fig. 12 Residuals r_1, r_2 and r_3 in actuator fault situation

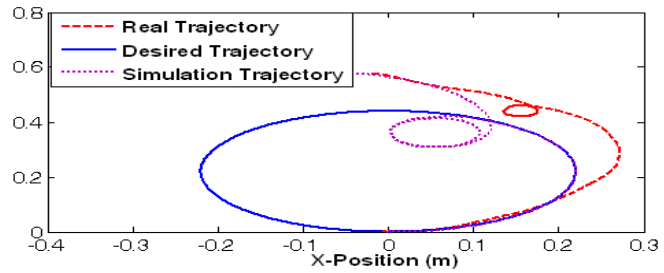

Fig. 13 Desired, simulated and real robot trajectories in faulty situation

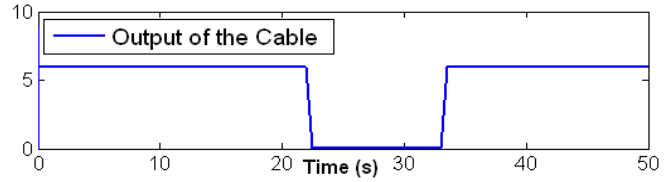

Fig. 14 Fault profile on the output signal of the cable

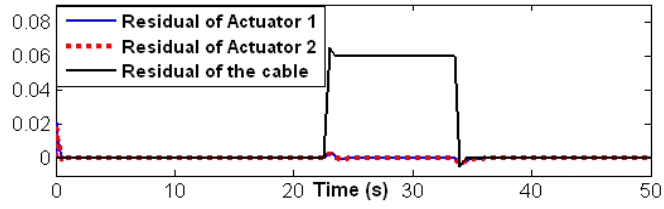

Fig. 15 Residuals r_1, r_2 and r_3 in transmission fault situation

5. CONCLUSION

In this paper, a model based fault detection and isolation applied on a mobile robot with transmission channel is presented. In this case, the transmission channel is considered as a complete and separate system from the robot, and the synthesized residuals show the isolability of the cable fault from the actuators faults as shown by the simulation and the experimental results. The use of a virtual simulator developed in this framework, demonstrates the principal role of this tool to help the system supervisor in predicting and/or detecting some major faults, which can be resolved according to the state of the situation by maintenance or control reconfiguration. In a perspective work, a study of the influence of the induced system delay and parameters uncertainties on the system performances will be an interesting step for diagnosis robustness increasing.

***Acknowledgements*:** The present research work was supported by Science and Technology for Safety in Transportation, and founded by the European Union, the Délégation Régionale à la Recherche et à la Technologie, the Ministère Délégué à l'Enseignement Supérieur et à la Recherche, the Région Nord Pas de Calais and the Centre National de la Recherche Scientifique.

REFERENCES

B. Ould Bouamama, A. K. Samantaray, M. Staroswiecki, and G. Dauphin-Tanguy, 'Derivation of constraint relations from bond graph models for fault detection and isolation', *International Conference on Bond Graph Modeling and Simulation (ICBGM'03), pages 104-109. Simulation Series Vol.35, No.2, ISBN 1-56555-257-1, 2003*.

C. Shannon, W. Weaver, 'The mathematical theory of communication', *University of Illinois Press, Urbana, 1949*.

E. Witrant, A. Van der Schaft, S. Stramigioli, 'A passive model for a nonhomogeneous transmission line', *Technical report, Universiteit Twente, Enschede, Netherlands, 2005*.

G. Miano, A. Mafucci, 'Transmission Lines and Lumped Circuits', *Academic Press Series in Electromagnetism, 2001*.

H. Ye, G. Wang, and S. X. Ding 'A New Parity Space Approach for Fault Detection Based on Stationary Wavelet Transform', *IEEE Teans. On Autom. Cont., Vol. 49, N°. 2, pp. 281-287, 2004*

J. F. Magni and P. Mouyon, 'On residual generation by observer and parity space approaches', *IEEE Trans. Autom. Control, vol. 39, no. 2, pp. 441--447, Feb. 1994.*

J. Nilsson, B. Bernhardsson, B. Wittenmark, 'Stochastic analysis and control of real-time systems with random time delays', *Automatica Vol. 34, 57-64, 1998.*

K-Team web site: www.k-team.com.

L. Teppoz, 'Commande d'un système de conversion de type VSC-HVDC. Stabilité-contrôle des perturbations', *PhD thesis, INPG, Grenoble, France, 2005*.

M. A. Djeziri, R. Merzouki, B. Ould-Bouamama, G. Dauphin-Tanguy, `Bond Graph Model Based For Robust Fault Diagnosis', *ACC'2007, American Control Conference, pp. 3017 - 3022, New York, USA, 2007.*

M. Staroswiecki and G. Comtet-Varga. Analytical redundancy relations for fault detection and isolation in algebraic dynamic systems. *Automatica, Vol. 37, pp. 687---699, 2001*.

R. Isermann, 'Supervision, fault detection and fault diagnosis methods - an introduction'. *Control Engineering Practice, Vol. 5, No. 5:639---652, 1997.*

R. Krtolica, U. Ozguner, H. Chan, H. Goktas, J. Winkelman, M. Liubakka, 'Stability of linear feedback systems with random communication delays', *International Journal of Control, Vol. 59, pp. 925-953, 1994.*

R. Merzouki, K. Medjaher, M. A. Djeziri, B. Ould-Bouamama, `Backlash Fault Detection in Mechatronics System', *MECHATRONICS IFAC Journal, Vol. 17, pp. 299-310, 2007.*

Y. Zheng, H. Fang, and H. O. Wang, (2006). Takagi--Sugeno Fuzzy-Model-Based Fault Detection for Networked Control Systems with Markov Delays. In *IEEE Trans. On Sys., Man, and Cyb.---Part B: CYBERNETICS, Vol. 36, N°. 4, pp. 924-929*.

Y. Zheng, H. Fang, and Y. Wang 'Kalman Filter Based FDI of Networked Control System', *Proceedings of the 5m World Congress on Intelligent Control and Automation, Hangzhou, pp. 1330-1333, P. R. China.2, 2004.*